Pure & Appl. Chem., Vol. 70, No. 10, pp. 2007–2014, 1998.
Printed in Great Britain.

Intrinsic barriers to the formation and reaction of carbocations

John P. Richard, Tina L. Amyes and Kathleen B. Williams

Department of Chemistry, University at Buffalo, SUNY, Buffalo, New York, 14260, U.S.A.

Abstract: The Marcus equation relates the activation barriers ($\Delta G^{\ddagger}$) for organic reactions to the overall thermodynamic driving force (ΔG°) and the intrinsic barrier Λ, which is the value of $\Delta G^{\ddagger}$ when $\Delta G^{\circ} = 0$. Most treatments of substituent effects on the rate and equilibrium constants for the reactions of structurally homologous organic substrates make the assumption that the intrinsic barrier Λ remains constant with changes in ΔG°. However, there is good evidence for the nucleophilic addition of solvent to carbocations $XArCH(R)^{+}$ that changes in the aromatic ring substituent X and the benzyl substituent R result in large changes in the intrinsic barrier. Evidence is presented that: (1) There is no significant work required for formation of the reactive complex for proton transfer from carboxylic acids to a homologous series of α-methoxystyrenes $XArC(OMe)=CH_2$. (2) There is a difference in the curvature of the energy surfaces for the reactant and product states that results in their intersection at a transition state in which proton transfer has proceeded *ca.* two-thirds of the way from RCO_2H to $XArC(OMe)=CH_2$.

INTRODUCTION

The Marcus equation in it simplest form (eq 1) provides a useful framework for discussion of the origin of the activation barriers to organic reactions (ref. 1), because it relates the magnitude of the barrier ($\Delta G^{\ddagger}$) to the following two relatively easily understood quantities that can either be measured by experiment or determined by calculation:

(1) The overall change in free energy (ΔG°), which depends upon the changes in chemical bonding that occur on proceeding from reactant to products. The value of ΔG° can sometimes be determined by experiment, and it may be calculated using ab initio methods with a degree of confidence that has grown steadily in recent years.

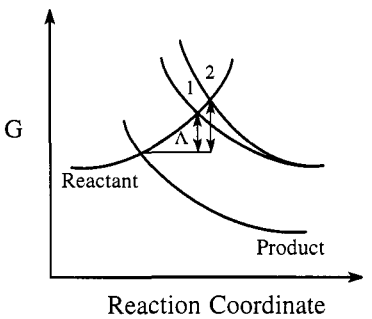

Figure 1. Free energy profiles for reactions in which there are changes in both thermodynamic driving force ΔG° and the intrinsic barrier Λ.

(2) The intrinsic barrier Λ (eq 1), which is the activation barrier in the absence of any thermodynamic driving force for the reaction ($\Delta G^{\circ} = 0$). Λ is usually assumed to remain constant with changes in ΔG° for reaction of a structurally homologous series of substrates. The size of Λ is determined by the energy required to effect the structural and electronic changes which occur on proceeding from ground to transition state, and it is reflected in the steepness of the approach of the energy surface to the transition state (Figure 1). The determination of Λ either by experiment (ref. 2) or by calculation (ref. 3) is more difficult than the determination of ΔG°.

*Lecture presented at the 14th International Conference on Physical Organic Chemistry, Florianópolis, Brazil, 21–26 August 1998. Other presentations are published in this issue, pp. 1933–2040.

$$\Delta G^{\ddagger} = \Lambda(1 + \Delta G^{\circ}/4\Lambda)^2 \qquad (1)$$

Eq 1 provides a starting point for the interpretation of substituent effects on the rate and equilibrium constants for organic reactions; however, this equation sometimes fails. These failures show that the constant parameter Λ and the variable ΔG° (eq 1) are often not sufficient to describe substituent effects on organic reactivity, and they suggest the need for a deeper consideration of the relationship between organic structure and reactivity.

We describe here failures of eq 1 to model the effect of changing substituents on the rate and equilibrium constants for nucleophilic addition to carbocations. In all cases these breakdowns of eq 1 can be accounted for by a straightforward consideration of the assumptions made in its derivation and use. In other words, these data provide support for the conclusion that Marcus theory provides a useful initial framework for the description and explanation of substituent effects on the reactions of carbocations.

THE MARCUS EQUATION

Marcus theory in its simplest form treats the free energy profiles for chemical reactions as pairs of symmetrical parabolas for the reactants and products which intersect at the transition state. The Marcus equation describes the position of the intersection of these parabolas ($\Delta G^{\ddagger}$) as a function of ΔG° and Λ. Several simplifying assumptions are made in the derivation and use of the Marcus equation (eq 1):

Figure 2. Free energy profiles for reactions in which: (A) There is a change in the thermodynamic driving force for a reaction with a constant Marcus intrinsic barrier. (B) Significant work must be performed on the free reactants and products to form complexes where a chemical reaction can occur. (C) There is a significant difference in the curvature of the free energy surfaces for the reactant and product states.

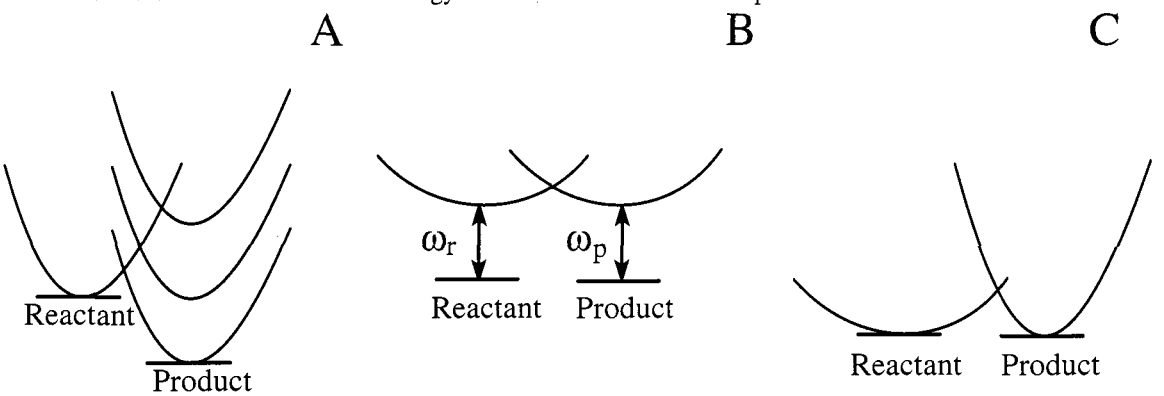

(1) It is generally assumed that changes in substituents at a series of structurally homologous substrates do not affect the intrinsic barrier Λ for the reaction (Figure 2A). The inadequacy of this assumption for the addition of nucleophiles to carbocations results in several interesting examples of the breakdown of the Marcus relationship which will be discussed in greater detail in the following section.

(2) The simple Marcus treatment assumes that the activation barrier for organic reactions is composed entirely of the barrier to the chemical transformation of the substrate to the transition state. More sophisticated treatments include terms for the work required for conversion of the reactants to a reactive complex (ω_r, Figure 2B) and for separation of the product complex to free products ($-\omega_p$) (ref. 1). We have carried out experiments designed to separate the *observed* barrier for the thermoneutral protonation of a homologous series of α-methoxystyrenes $XArC(OMe)=CH_2$ to give the corresponding α-alkoxy carbocations $XArC(OMe)CH_3^+$ into an intrinsic barrier Λ and a work term ω_r.

(3) Identical shapes are assumed for the parabolic free energy surfaces which describe the changes in

energy as the structures of the reactant and product approach that of the reaction transition state, so that the transition state for a thermoneutral reaction lies midway between reactants and products. We consider here the possibility that there are significant differences in the shapes of the free energy surfaces for the reactant and product states for protonation of $XArCH(OMe)CH_3^+$ by carboxylic acids, as illustrated by Figure 2C.

NUCLEOPHILIC ADDITION TO CARBOCATIONS

There is good evidence that the Marcus intrinsic barrier for the addition of nucleophiles to ring-substituted benzyl carbocations increases with increasing carbocation stabilization by resonance electron donation from the aromatic ring to the benzylic carbon (ref. 4). An intuitive explanation for this effect on the intrinsic barrier is that there is an energy cost for "relocalization" of electron density at the aromatic ring on proceeding from the delocalized carbocation to the transition state for nucleophile addition. More rigorous models have been developed to rationalize these and the related increases in the intrinsic barrier for the protonation of carbanions with increasing carbanion stabilization by resonance delocalization of negative charge onto electron-withdrawing substituents (refs. 5, 6). This tendency of the intrinsic barrier for nucleophilic addition to benzylic carbocations to increase with increasing carbocation stabilization by resonance manifests itself in interesting rate-equilibrium relationships for these reactions.

Figure 3. (A) Hypothetical free energy profiles for the addition of solvent to $4\text{-}MeOArCH(CH_3)^+$ and $4\text{-}Me_2NArCH(CH_3)^+$. **1** is the barrier for a reaction in which Λ remains constant and **2** is the barrier for a reaction in which there is an increase in Λ. (B) Hypothetical free energy profiles for the addition of solvent to 4-MeOArCH(R)+ where there is an increase in the activation barrier from **3** to **4** that is attributable to the increase in the intrinsic reaction barrier that occurs with *increasing* thermodynamic driving force for the reaction.

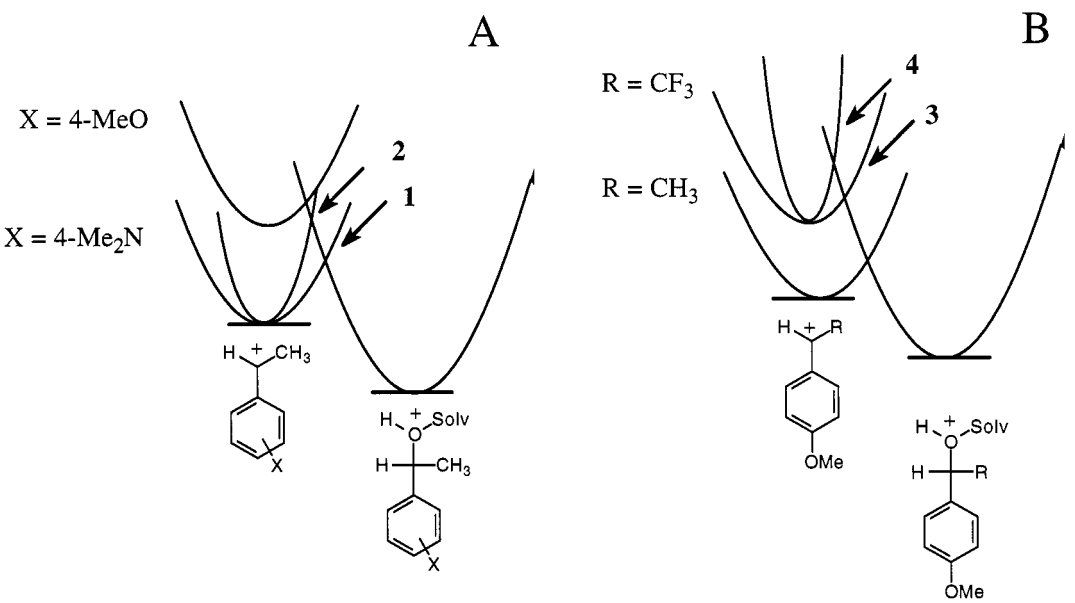

(1) The rate constant k_s (s^{-1}) for the reaction of carbocations $XArCH(CH_3)^+$ with a solvent of 50:50 (v:v) trifluoroethanol/water decreases by *ca.* 10^8-fold for the change from X = 4-Me ($k_s = 6 \times 10^9$ s^{-1}) (ref. 7) to X = $4\text{-}Me_2N$ ($k_s = 40$ s^{-1}) (ref. 8). An analysis of the resonance and polar substituent effects on the rate and equilibrium constants for the addition of water to $XArCH(CH_3)$+ shows that 53% of the equilibrium resonance substituent effect is expressed at the transition state for the addition of water to the carbocation, but that only 36% of the polar substituent effect is expressed at this transition state (ref. 7). These results show that the stabilization of $XArCH(CH_3)^+$ by resonance electron-donating substituents results in a larger increase in the activation barrier to solvent addition than is observed for an equal stabilization of the carbocation by polar

electron-donating substituents. They are consistent with the energy profiles shown in Figure 3A. The 4-Me_2N for 4-MeO substitution at $XArCH(CH_3)^+$ would result in an increase in the activation barrier to **1** if the curvature of the reaction coordinate remains constant, as is proposed to occur for changes in polar ring substituents. However, there is an additional increase in the activation barrier, to **2**, due to an increase in the intrinsic barrier Λ, which is manifested as the relatively large 53% expression of the resonance effect of the 4-Me_2N substituent at the transition state for nucleophilic addition of water.

(2) The rate constant for the reaction of carbocations 4-MeOArCH(R)$^+$ with solvent remains almost constant ($k_s \approx 5 \times 10^7$ s^{-1} in 50:50 (v:v) trifluoroethanol/water) as the α-substituent R is changed from strongly electron-donating (α-OMe) to strongly electron-withdrawing (α-CF_3) (ref. 9). This change in R results in a *ca.* 19 kcal/mol destabilization 4-MeOArCH(R)$^+$ relative to the neutral azide ion adducts (ref. 9). A change in substituent which results in an increased driving force for a reaction (*e.g.*, R = OMe to R = CF_3, Figure 3B) normally leads to a decrease in the activation barrier. By contrast, the constant values of k_s across the series of 4-MeOArCH(R)$^+$ suggest that this "normal" substituent effect is masked by an opposing substituent effect which results in an increase in the activation barrier (refs. 4, 9).

The change from electron-donating α-substituents R at 4-MeOArCH(R)$^+$ (*e.g.*, α-OMe), which stabilize positive charge at the benzylic carbon, to electron-withdrawing substituents such as α-CF_3, which create a destabilizing charge-dipole interaction results in a progressive increase in the delocalization of positive charge onto the 4-methoxyphenyl ring (ref. 10). This is because delocalization of positive charge onto the aromatic ring reduces the resonance stabilization by α-OMe in one case, and in the other it serves to attenuate the destabilizing polar interactions of the α-CF_3 group by increasing the separation of this group from the formal center of positive charge. The increase in carbocation stabilization by charge delocalization onto the 4-methoxyphenyl ring results in an increase in the intrinsic barrier Λ for the nucleophilic addition reaction (ref. 4). This is shown in Figure 3B as the change from a coordinate that passes through transition state **3** to the steeper coordinate which passes through transition state **4**. We have proposed that the increases in the activation barrier for the reaction of 4-MeOArCH(R)$^+$ that result from changes in Λ approximately cancel the decreases in this barrier resulting from the increased thermodynamic driving force, with the net effect that $\Delta G^{\ddagger}$ is independent of R (ref. 9).

In summary, the different changes in k_s (s^{-1}) observed as the thermodynamic stability of XArCH(R)$^+$ is changed by varying the ring substituent X (k_s increases with decreasing stability) and the α-substituent R (k_s remains roughly constant) reflect the different effect of these substituents on the intrinsic reaction barrier Λ. The value of Λ increases as XArCH(R)$^+$ is stabilized by varying X, but decreases as the carbocation is stabilized by changing R (Figure 3). In the first case the effects of changing ΔG° and Λ on the activation barrier reinforce each other, but in the second case they oppose each other and, fortuitously, cancel. These results show that when formulating explanations for substituent effects on organic reactions it is important to consider explicitly the effect of changing substituent on both the thermodynamic driving force for the reaction ($\Delta\Delta G^{\circ}$) and the intrinsic reaction barrier ($\Delta\Lambda$). When the latter effect is very large it may dominate the observed substituent effect on organic reactivity.

INTRINSIC BARRIERS TO THE REACTIONS OF CARBOCATIONS

In order to provide a quantitative framework upon which to base discussions of the relationship between the observed and the intrinsic activation barriers to the addition of nucleophiles to carbocations, we have examined

Scheme 1

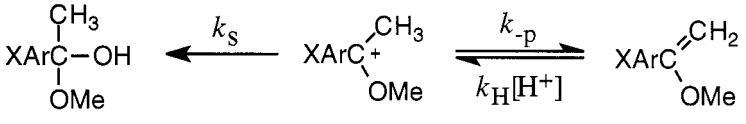

the intrinsic barriers Λ for the deprotonation of α-alkoxy carbocations $XArC(OMe)CH_3^+$ to give α-methoxystyrenes $XArC(OMe)=CH_2$ (Scheme 1).

We evaluated the rate and equilibrium constants for the reactions of $XArC(OMe)CH_3^+$ shown in Scheme 1 as follows: (a) The second-order rate constant for protonation of $PhC(OMe)=CH_2$ by hydronium ion, $k_H = 79$ M^{-1} s^{-1}, was determined by monitoring the conversion of α-methoxystyrene to acetophenone. (b) The rate constant for reaction of $PhC(OMe)CH_3^+$ with solvent water, $k_s = 5 \times 10^7$ s^{-1}, was determined in earlier work (ref. 11). (c) A value of $k_{-p}/k_s = 6 \times 10^{-5}$ for partitioning of $PhC(OMe)CH_3^+$ [generated by acid-catalyzed cleavage of $PhC(OMe)_2CH_3$] between loss of a proton and addition of solvent water was determined from the ratio of the yields of the products of these reactions. Combining the values of k_{-p}/k_s and k_s gives $k_{-p} = 3000$ s^{-1} for deprotonation of $PhC(OMe)CH_3^+$ by solvent water. The resulting acidity constant of the carbon acid $PhC(OMe)CH_3^+$, calculated as $K_{CH} = k_{-p}/k_H = 40$ M ($pK_{CH} = -1.6$) is in fair agreement with the literature value of $K_{CH} = 65$ M determined by a different experimental protocol (ref. 12).

The intrinsic rate constant of $(k_H)_o = (k_{-p})_o = 47$ s^{-1} for thermoneutral protonation of $XArC(OMe)=CH_2$ by hydronium ion to give $XArC(OMe)CH_3^+$ was determined by interpolation of a linear plot of log k_H (M^{-1} s^{-1}) against log K_{CH} (ref. 12) to log $K_{CH} = 0$. This intrinsic rate constant corresponds to an activation barrier of 15 kcal/mol, which is similar to values reported in other studies of the protonation of vinyl ethers (refs. 12, 13, 14).

WORK AND OTHER CONSIDERATIONS.

The composition of the barrier to the thermoneutral protonation of vinyl ethers is of current topical interest. This is because the published reports that the intrinsic barrier Λ for deprotonation of ketones (eq 2) is substantially larger than that for deprotonation of α-alkoxy carbocations (eq 3) have prompted the proposal that proton transfer to an enzyme-bound carbonyl group will result in a decrease in the intrinsic barrier for deprotonation of the α-carbon (eq 4) and contribute to the enzymatic rate acceleration for this reaction (ref. 15).

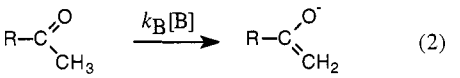

(2)

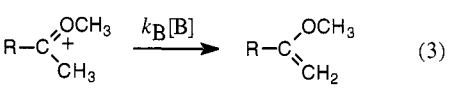

(3)

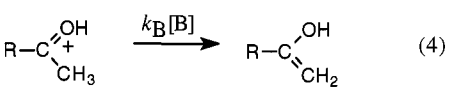

(4)

This intriguing mechanism for transition state stabilization by Brønsted acid catalysis of proton transfer deserves careful consideration. An examination of literature shows that there is, in fact, little difference in the observed activation barrier to the thermoneutral deprotonation of ketones (*ca.* 12 kcal/mol) (ref. 2) and protonation of vinyl ethers by hydronium ion (*ca.* 15 kcal/mol, this is the microscopic reverse of deprotonation of α-alkoxy carbocations) (refs. 12, 13, 14). However, for the former reaction (eq 2), the observed barrier for thermoneutral proton transfer was taken as being equal to the intrinsic barrier Λ ($\omega_r = 0$, Figure 2B), while for the latter reaction (eq 3), the observed barrier for thermoneutral reaction was separated into a work term of $\omega_r \approx$ 12 kcal/mol, and a chemical intrinsic barrier of $\Lambda \approx 3$ kcal/mol, so that $\omega_r + \Lambda = 15$ kcal/mol is equal to the overall barrier for the thermoneutral reaction (Figure 2B). While there was some justification for the different treatments of the experimental data for the reactions of ketones (eq 2) and vinyl ethers (eq 3), it is not clear whether there were sufficient experimental data for a rigorous separation of the observed activation barrier for thermoneutral protonation of vinyl ethers into an intrinsic barrier Λ and a work term ω_r. Also, it is not obvious why different amounts of work should be required to bring a free ketone and a free vinyl ether into a conformation/complex where a chemical reaction can occur.

The free energy reaction coordinate profiles for reactions with intrinsic barriers of 3 and 15 kcal/mol have dramatically different forms that can be distinguished by experiment. Figure 4A shows the profile for a thermoneutral reaction with a large Marcus intrinsic barrier of $\Lambda = 15$ kcal/mol and no work term ($\omega_r = 0$).

Similarly, Figure 4B shows the profile for a thermoneutral reaction with a large work term for formation of a reactive complex ($\omega_r > 0$) and a small Marcus intrinsic barrier (Λ) to the actual chemical step, which is constructed from the intersection of two parabolas of shallow curvature. The different curvatures of the free energy profiles for proton transfer reactions that have a large intrinsic barrier (steep curvature, Figure 4A) and a small intrinsic barrier (shallow curvature, Figure 4B) result in markedly different *changes* in the position of the transition state along the reaction coordinate with changing thermodynamic driving force for the reaction. This is illustrated in Figure 4A for a reaction with a large intrinsic barrier that shows small changes in the position of the transition state with changing thermodynamic driving force, and in Figure 4B for a reaction with a small intrinsic barrier that shows much larger changes in transition state structure.

Figure 4. Free energy reaction coordinate profiles for the protonation of α-methoxystyrenes (vinyl ethers). (A) A reaction with a large Marcus intrinsic barrier Λ and no work terms. (B) A reaction with a small Marcus intrinsic barrier and large work terms $\omega_r = \omega_p > 0$.

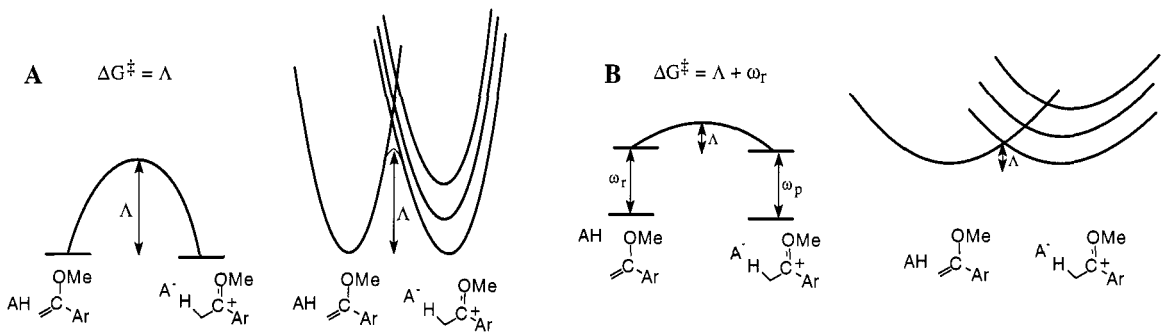

The approximate position of the transition state for proton transfer can be determined as the Brønsted coefficient, $\alpha = \partial \log k_{HA}/\partial pK_{HA}$, where k_{HA} is the second-order rate constant for proton transfer to the α-methoxystyrene, and K_{HA} is the acidity constant of the Brønsted acid. The Brønsted coefficient is also equal to the first derivative of the full Marcus equation containing work terms for both the reactants and the products (eqs 5 and 6). The intrinsic barrier to proton transfer can be estimated from the *change* in the position of the transition state ($\partial\alpha$) with changing thermodynamic driving force for the reaction (∂pK_{CH}, where pK_{CH} is the pK_a of the product α-alkoxy carbocation), because the second derivative of the Marcus equation (eq 7) *is inversely proportional to the intrinsic barrier* Λ . The determination of Marcus intrinsic barriers by this method has the advantage that it is independent of the magnitude of the work terms ω_r and ω_p, because these quantities drop out on taking the second derivative of the Marcus equation (eq 7).

$$\Delta G^{\ddagger} = \omega_r + \Lambda\left(1 + \frac{(\Delta G_o)_{obsd} - \omega_r + \omega_p}{4\Lambda}\right)^2 \qquad (5)$$

$$\alpha = \frac{\partial \log k_{HA}}{\partial pK_{HA}} = 0.5 + \frac{(\Delta G_o)_{obsd} - \omega_r + \omega_p}{8\Lambda} \qquad (6)$$

$$\frac{\partial \alpha}{\partial pK_{CH}} = \frac{\partial^2 \log k_{HA}}{\partial pK_{HA}\partial pK_{CH}} = \frac{-2.303RT}{8\Lambda} \qquad (7)$$

We have evaluated the intrinsic barrier to the protonation of $XArC(OMe)=CH_2$ by determining the change, with changing thermodynamic driving force for proton transfer, in the Brønsted coefficient α for the reactions of carboxylic acids and H_3O^+. The change in the value of α is shown in plots of log $[(k_{HA})_X/(k_{HA})_{4\text{-}NO2}]$ against the acidity of the Brønsted acid, pK_{HA} (Figure 5). In this Figure, the rate constants for protonation of

XArC(OMe)=CH_2, $(k_{HA})_X$, have been normalized by dividing by $(k_{HA})_{4\text{-}NO2}$, the rate constant for protonation of the reference substrate 4-NO_2ArC(OMe)=CH_2 by the same Brønsted acid. This minimizes the systematic deviations observed in traditional Brønsted plots of log k_{HA} against pK_{HA}. The slopes of the plots in Figure 5 are equal to the *difference* in the Brønsted coefficient α for protonation of 4-NO_2ArC(OMe)=CH_2 and XArC(OMe)=CH_2, $\alpha_{4\text{-}NO2} - \alpha_X$. The plot of $\alpha_{4\text{-}NO2} - \alpha_X$ against pK_{CH} for the product carbon acid (not shown) has a slope of 0.016 ± 0.02, which is consistent with a range of intrinsic barriers of 9 kcal/mol < Λ < 12 kcal/mol. The data are clearly inconsistent with a small intrinsic barrier of $\Lambda \approx 3$ kcal/mol for this reaction, but these barriers are very similar to the observed barrier of 13 kcal/mol for the thermoneutral protonation of XArC(OMe)=CH_2 by carboxylic acids. We conclude that the work required to form the reactive complex containing the substrate is relatively small, and that most of the activation barrier for this thermoneutral proton transfer reaction is associated with movement along the reaction coordinate to the reaction transition state (Figure 4A).

Figure 5. Semi-logarithmic plots of normalized rate constants $(k_{HA})_X/(k_{HA})_{4\text{-}NO2}$ for the protonation of XArC(OMe)=CH_2 by carboxylic acids against the pK_a of the acid: (●), X = 4-MeO; (▼), X = H; (■), X = 4-NO_2; (▲), X = 3,5-di-NO_2.

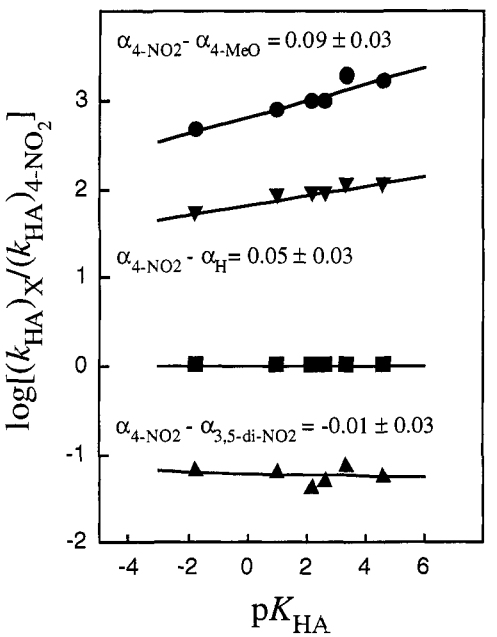

Figure 6. Semi-logarithmic plot of rate constants k_{HA} for the protonation of XArC(OMe)=CH_2 by carboxylic acids against the pK_a of the acid: (●), X = 4-MeO; (▼), X = H; (■), X = 4-NO_2; (▲), X = 3,5-di-NO_2.

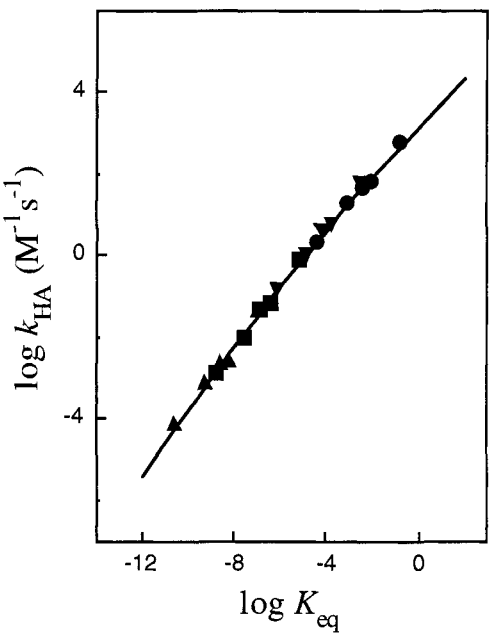

Figure 6 shows a plot of log k_{HA} for protonation of XArC(OMe)=CH_2 by carboxylic acids against the equilibrium constant log K_{eq} for the proton transfer reaction. The small curvature in this plot is inconsistent with an intrinsic barrier of 2 - 4 kcal/mol but is consistent with an intrinsic barrier of 10 kcal/mol. The solid line through the data in Figure 6 shows the fit to the full Marcus equation using values of Λ = 9, ω_r = 0 and ω_p = 7 kcal/mol. Extrapolation of this fit to ΔG° = 0 gives an intrinsic rate constant of k_{HA} = 1500 M^{-1} s^{-1} and a tangential slope at ΔG° = 0 of α = 0.66. This is substantially larger than α = 0.50 for a thermoneutral reaction that is required by the simple Marcus equation (eq 1). While this fit is acceptable, it is not obvious why there should be a large difference in the work terms for formation of the reactant and product complexes. Our results can be more sensibly explained by a significantly smaller degree of curvature along the free energy surface near the reactants, which involves primarily stretching of the O-H bond of a carboxylic acid, than of the energy surface near the products, which involves primarily stretching of the C-H bond of the α-alkoxy carbocation (Figure 2C). Such an asymmetric energy surface is consistent with the notion that the energy surface near the reactants involves mainly proton transfer from the electronegative oxygen atom, while the energy surface near

the products involves mainly proton transfer from carbon. This should result in shallow curvature of the energy surface near the reactants, as a result of the relatively small intrinsic barriers to proton transfer at oxygen (ref. 16), but steeper curvature of the energy surface near the products, as a result of the relatively large intrinsic barriers to proton transfer at carbon (ref. 3).

ACKNOWLEDGEMENTS

We acknowledge the National Institutes of Health (Grant GM 39754) for support of this work.

REFERENCES

1. R. A. Marcus, *J. Phys. Chem.* **72**, 891-899 (1968).
2. J. P. Guthrie, *Can. J. Chem.* **74**, 1283-1296 (1996).
3. W. H. Saunders, *J. Am. Chem. Soc.* **116**, 5400-5404 (1994).
4. J. P. Richard, *Tetrahedron* **51**, 1535-1573 (1995).
5. C. F. Bernasconi, *Adv. Phys. Org. Chem.* **27**, 119-238 (1992).
6. C. F. Bernasconi, *Tetrahedron* **41**, 3219-3234 (1985).
7. J. P. Richard, M. E. Rothenberg, W. P. Jencks, *J. Am. Chem. Soc.* **106**, 1361-1372 (1984).
8. F. L. Cozens, N. Mathivanan, R. A. McClelland, S. Steenken, *J. Chem. Soc., Perkin Trans. 2*, 2083-2090 (1992).
9. T. L. Amyes, I. W. Stevens, J. P. Richard, *J. Org. Chem.* **58**, 6057-6066 (1993).
10. I. Lee, D. S. Chung, H. J. Jung, *Tetrahedron* **50**, 7981-7986 (1994).
11. T. L. Amyes, W. P. Jencks, *J. Am. Chem. Soc.* **111**, 7888-7900 (1989).
12. J. Toullec, *J. Chem. Soc., Perkin Trans. 2*, 167-171 (1989).
13. W. K. Chwang, R. Eliason, A. J. Kresge, *J. Am. Chem. Soc.* **99**, 805-808 (1977).
14. A. J. Kresge, D. S. Sagatys, H. L. Chen, *J. Am. Chem. Soc.* **99**, 7228-7233 (1977).
15. J. A. Gerlt, P. G. Gassman, *J. Am. Chem. Soc.* **115**, 11552-11568 (1993).
16. M. Eigen, *Angew. Chem., Int. Ed. Engl.* **3**, 1-72 (1964).